A near-infrared SETI experiment: commissioning, data analysis, and performance results

Conference Paper · August 2016

DOI: 10.1117/12.2232861

A near-infrared SETI experiment: commissioning, data analysis, and performance results

Jérôme Maire[a], Shelley A. Wright[b,c], Patrick Dorval[a], Frank D. Drake[d], Andres Duenas[b], Howard Isaacson[e,f], Geoffrey W. Marcy[e], Andrew Siemion[e,f], Remington P. S. Stone[g], Melisa Tallis[b], Richard R. Treffers[h], and Dan Werthimer[e,f]

[a] Dunlap Institute for Astronomy and Astrophysics, University of Toronto, ON, Canada;
[b] Department of Physics, University of California San Diego, CA, USA;
[c] Center for Astrophysics and Space Sciences, University of California San Diego, CA, USA;
[d]SETI Institute, Mountain View, CA, USA
[e]Astronomy Department, University of California Berkeley, CA, USA;
[f]Space Sciences Laboratory, University of California Berkeley, CA, USA;
[g]Lick Observatory, University of California Observatories, Mt. Hamilton, CA, USA;
[h]Starman Systems, LLC, Alamo, CA, USA

ABSTRACT

Over the last two decades, optical Search for Extra-Terrestrial Intelligence (SETI) experiments have focused on either detecting continuous or pulsed lasers that could be used for interstellar communication or energy transmission. Near-infrared offers a compelling window for signal transmission since there is a decrease in both interstellar extinction and Galactic background compared to optical wavelengths. An innovative Near-InfraRed and Optical SETI (NIROSETI) instrument has been designed and constructed to take advantage of a new generation of fast (> 1 Ghz) low-noise near-infrared (850 - 1650 nm) avalanche photodiodes to search for nanosecond pulses. The instrument was successfully installed and commissioned at the Nickel 1-m telescope at Lick Observatory in March 2015. We describe the overall design of the instrument and the methods developed for data acquisition and reductions. Time and height analyses of the pulses produced by the detectors are performed to search for signal periodicities and coincidences. We also discuss the NIROSETI survey target list and observing procedures.

Keywords: SETI, Optical SETI, High Time Resolution Instruments, Near Infrared Instrumentation

1. INTRODUCTION

A new generation of fast (> 1 GHz) wide-bandwidth InGaAs avalanche photodiode (APD) detectors that use Internal Discrete Amplification (IDA) technology,[1,2] with ultra-low noise (below 10^6 counts per second), have created new opportunities for astronomical high-time resolution observations in the near-infrared regime. Fast astronomical events such as transients, luminosity fluctuations of variable stars, and pulsar emission can be better characterized using high-precision timing at near-infrared wavelengths. Near-infrared SETI that focuses on detecting short (< nanosecond) pulsed laser emission became possible with this new family of APD detectors that are capable of scanning J- and H-bands simultaneously.

Even though several SETI radio[3,4] and optical[5–11] experiments have been performed in the last few decades, wide regions of the electromagnetic spectrum, including the infrared regime remain largely unexplored. Interstellar communication at near-infrared wavelengths have several advantages over other wavelength regimes. Propagation of light through the ionized component of the interstellar dispersive medium (e.g. free electrons), gives rise to interstellar extinction which is significantly lower in the near-infrared than in the visible,[12] hence

Further author information: (Send correspondence to J.M. or S.A.W.)
J.M.: E-mail: maire@dunlap.utoronto.ca
S.A.W..: E-mail: saw@physics.ucsd.edu

extending the distance at which an emitter could be detected with respect to visible wavelength. This opens a window for near-infrared SETI observations through the galactic plane and dusty environments at the Galactic Center. Light scattering can affect pulse widths, setting a limit to the time resolution observations, especially for long wavelengths and radio pulse detection, but this effect is negligible for optical near-infrared wavelengths at nanosecond timescales.[8]

Pulsed and continuous wave laser intensities have increased by several orders of magnitude in the last decades. Current pulsed lasers, for instance the Japanese LFEX device[*] or the National Ignition Facility[†] from Lawrence Livermore National Laboratory, can produce optical pulses with 2 petawatts (2.10^{15}W) peak power for a duration of a few picoseconds (10^{-12}s). With today's laser technology, the most powerful laser pulse would be able to outshine our sun by several orders of magnitude over large interstellar distances.[8] Some projects, such as the European Extreme Light Infrastructure,[13] aims to build exawatt class lasers (10^{18}W) that will deliver extremely bright pulses at 2μm wavelength by producing kiloJoules of power over 10 femtoseconds (10^{-14}s). Such pulsed signals at nanosecond (or faster) intervals may be distinguishable from most known astrophysical sources if observed with a high-time resolution instrument.

In this paper we describe the recent deployment of the first near-infrared SETI survey using the NIROSETI[12] instrument. An overview of the instrument is outlined in Section 2. Data analysis techniques are described in Section 3. Commissioning of the instrument and SETI survey status are summarized in Sections 4 and 5.

2. INSTRUMENT OVERVIEW

The NIROSETI instrument[12] is a high-time resolution instrument designed to perform a SETI targeted survey to search for near-infrared (950nm to 1650nm) nanosecond pulses. The instrument includes two detectors that simultaneously observes the same portion of the sky, which minimizes the probability of false detection that could be generated by various sources of noise. The instrument is located at the Cassegrain focus of the Nickel telescope (1m) at Lick Observatory. The conceptual design of the instrument is based upon a predecessor Lick Optical SETI instrument,[9,14] a nanosecond pulse finder observing in the visible regime.

NIROSETI optical and mechanical designs were optimized to ensure that it operates with high sensitivity and ease in detector alignment and modularity (the instrument can operate with one or two detectors). For calibration and system verification, a near-infrared (980 nm) pulsed laser source was designed and incorporated in the instrument. The main parameters characterizing the instrument are reported in Table 1.

As shown on Fig.1, the visible light collected by the Nickel telescope is focused on the guider camera, while the near-infrared light is reflected by a dichroic towards a 50:50 split-ratio beam splitter that divides the light between two IDA APD detectors, cooled at -25°C. Detectors are held on the base plate of the instrument by kinematic mounts and stages for accurate alignment on the optical axis. These two InGaAs photo-diodes are designed for analog detection of extremely low-level light signals (from one photon to several thousand photons per pulse).[1,2] Biased at high-voltage ($\sim$60V), these detectors require very low μA current with small 10μA compliance that is supplied by specifically-designed high-voltage low-current power-supplies built at Space Science Laboratory, Berkeley. At low-light levels, the voltage height of a photo-event pulse generated on an IDA detector is linearly proportional to the number of photons in that pulse.[1,2]

The choice of two detectors was determined to minimize the probability of false positives that could be generated by detector noise, cosmic-rays, and Poisson statistics from stellar photon rate. Indeed, these events are unlikely to occur within the same nanosecond on both detectors. Increasing the number of detectors in this configuration is at the expense of the sensitivity of the instrument, and it can be shown[15] that at the low-level light regime, observing with two detectors is a good trade-off between sensitivity and minimization of false positives. The instrument can also observe with a single detector by moving the beam-splitter out of the optical axis to maximize the sensitivity of the instrument at the expense of a higher false positive rate.

In order to align our selected sources with the 200μm near-infrared detectors, an optical guider camera (Pointgrey Grasshopper) has been integrated into the NIROSETI instrument. With its 2x2.5 arcmin field-of-view, the guider camera is used before and during each acquisition to accurately center the observed object onto a

*http://www.eurekalert.org/pub_releases/2015-08/ou-wpl080615.php

†https://lasers.llnl.gov/

Table 1: NIROSETI instrument main characteristics.

Telescope	1-m. f/17 Nickel Telescope
Detectors	4GHz InGaAs NIR-DAPDs from Amplification Technologies Inc.
Detector Size	200μm
Detector Cooling	-25°C
High-Voltage, micro-Amp Power Supply	60V bias, $\sim 2\mu$A current from Berkeley SETI Research Center
Instr. Sensitivity	380 photons/m^2/pulse
Computer	Sun Fire X4150
Guider Camera	Sony ICX694 CCD PGE 60S6M-C 6.0Mpix

Observations	Targeted, ns-μs pulse detection
Wavelengths	from 0.9μm to 1.75μm simultaneously (J, H-bands)
Pulse width	0.4ns
Field-of-view	2.5 arcsec
Source Unit	0.98μm pulsed laser, 10ns pulse width, 4.6MHz duty cycle
Oscilloscope	2.25GHz 8 GSa/s 54846B Agilent
Controllers	Thorlabs TTC001, TLD001, MTS50-Z8
Guider Camera FoV & plate scale	154 x 123 arcsec, 0.056 arcsec

3-arcsec reference position that matches the optical axis of the near-infrared detectors. For extended objects, such as globular clusters and galaxies, multiple observations are performed with multiple telescope offsets positions on the source for each data acquisition. Using the guide camera 30 second maximal exposure time, objects as faint as 18th magnitude were observed in single frames with the Nickel telescope.

The instrument is also equipped with an internal source unit for testing the sensitivity of the instrument. This source unit includes a 0.98μm laser diode with a pigtailed fiber and collimation optics that mimic the focal ratio of the telescope. A pulser was designed to modulate the laser diode emission in order to produce 10ns-width pulses at variable MHz duty cycles.

The analog signals coming from the detectors are amplified with high-bandwidth amplifiers, and voltages are measured using a 2.25 GHz Agilent oscilloscope with a maximal time resolution of 4 GSa/s per channel. Waveforms are sent to a Sun Fire computer for signal processing and analysis. Acquisition software was custom-designed to record high time resolution waveforms and interact with the telescope. This software aids in detector alignment and controls instrument components: detector shutters, temperature controllers, internal pulsed source unit, beam-splitter stage, guider camera, oscilloscope and power supplies. This software has been designed to help observers to perform on-sky acquisitions and to take necessary calibrations and performance tests with the instrument.

Real-time data processing is performed on each detector waveform by analysing the pulse height and arrival time of each pulse. The software searches for abnormal high-voltage (many photons) coincident pulses and performs a periodicity search using temporal waveform periodograms. In real-time, results are summarized to the observer on a panel of indicators which quantify how unlikely were the occurrences of measured pulse heights and coincidence events (section 3). Alarm thresholds are set on these indicators to alert observers of a potential signal unlikely to have been generated by detector noise or star photo-detections.

For each target acquisition, a report is generated that includes object characteristics, weather conditions, observer comments, telescope and instrument settings, detector alignment verification, display of waveforms, record of the highest pulses and coincidence events, full pulse height distributions, periodograms and alarm indicators. At the end of the night, an automatic summary of all targets observed are generated that contain links to each individual observed object report. A target database which contains the main characteristics of the objects selected for the survey has been implemented, and is automatically updated after each acquisition to include reports and re-observing relevance. Observations can be performed at the summit or entirely from remote sites.

3. DATA ANALYSIS

Searching for nanosecond pulses represents a significant challenge with the amount of data flow and storage rate. To tackle the issue of managing large amounts of data, acquisitions are divided into two operational

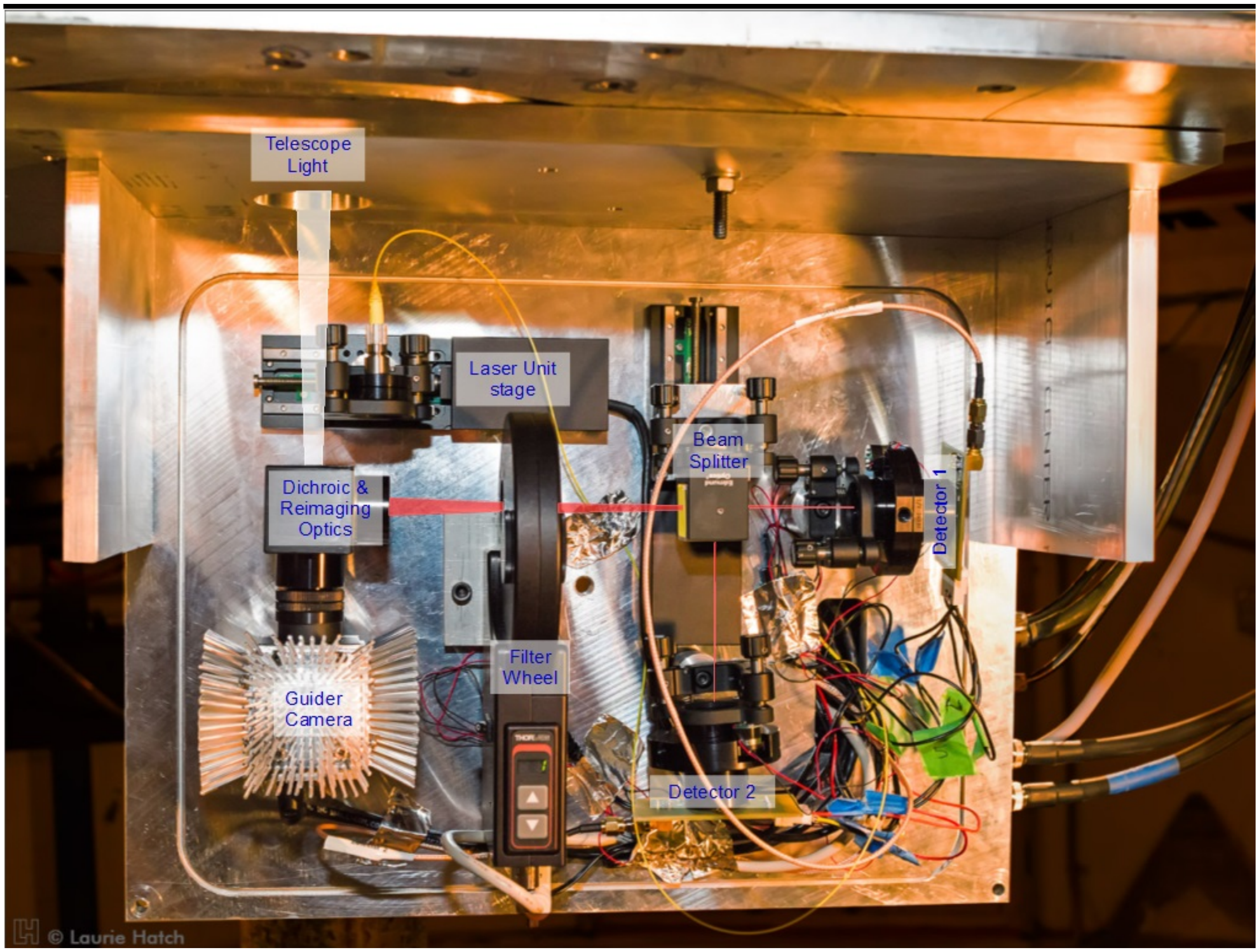

Figure 1: The optical bench of the NIROSETI instrument is shown with cover removed. The light of the observed object (white and red drawing over-plotted) is collected by the telescope and sent through the entrance of the instrument (upper left). The visible light is focused onto the guider camera while a dichroic reflects the near-infrared light towards a 50:50 beam splitter that divides the light between two detectors. (Picture credit: © Laurie Hatch Photography)

modes. First, a waveform acquisition is performed by recording 0.2-ms detector waveforms to conduct a full data analysis. Fig.2 (left panel) represents a part of those typical waveforms generated by the detectors that shows several sub-nanosecond pulses which may be generated by photo-events. Second, during a 300-second data acquisition, the oscilloscope is set to only trigger an acquisition when a pulse with large amplitude ($>$ 45mV, i.e. a few dozen photons per pulse) is measured on the channel corresponding to the first detector. Each trigger event activates the record of 40ns-long detector waveforms as shown on Fig.2 (right panel).

3.1 PULSE HEIGHT DISTRIBUTION

For each target, we perform a pulse height distribution (PHD) analysis that is intended to detect the highest pulses per acquisition, and to identify abnormal numbers of pulse occurrences that deviate from dark and stellar PHD observations.

To determine the pulse arrival time and height, waveforms are smoothed with a one-nanosecond boxcar window to reduce noise effects. Pulses are then detected in the smoothed waveforms using first-derivative tests. The PHD is then calculated by measuring the number of pulses per second above a given threshold voltage.

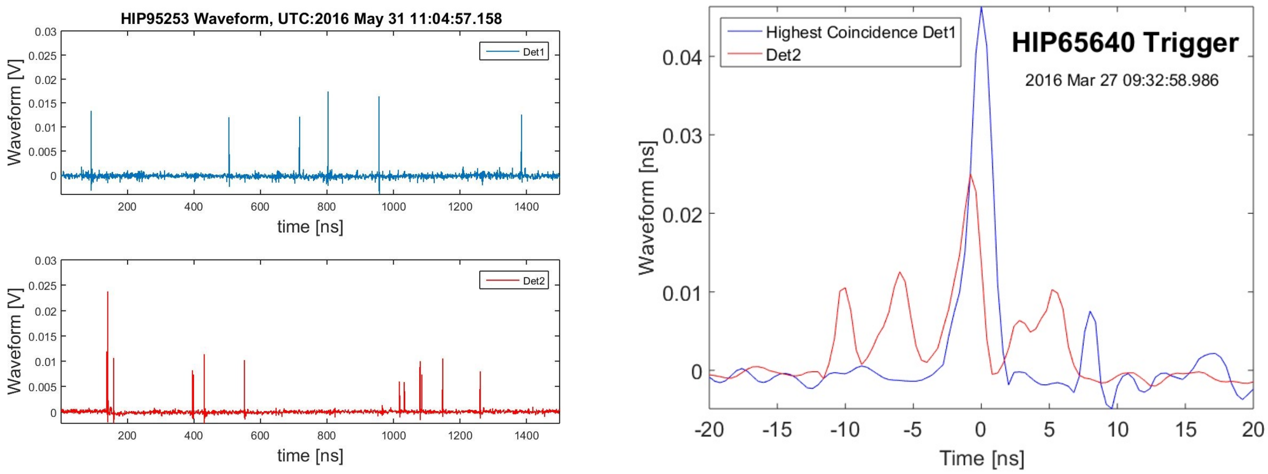

Figure 2: Left: Typical detector waveforms acquired with the two near-infrared detectors of the NIROSETI instrument. Pulses of $\sim 5-30$mV amplitudes are generated by either photo-events or detector noise. Right: Waveforms acquired during a trigger event that was generated by the detection of a high pulse on detector 1, along with the simultaneous waveform on detector 2.

Once acquired, PHDs are compared to previous dark acquisitions (Fig.3). The highest ratio of these PHDs are reported to observers in real-time to detect abnormal pulse height occurrence.

A second indicator, also related to PHD analysis, measures how long it would have taken on average to obtain the highest pulses found on both channels if they were due to either a detector noise event or a detection of stellar photons. Measured PHDs exhibit an exponential behavior (linear on the semi-log scale of Fig.3) that characterizes the number of pulse height occurrences. We extrapolate this exponential relationship to the voltage of the highest detected pulses to determine the average number of occurrences of such events if due to detector noise or star photo-detections.

3.2 COINCIDENCE BETWEEN DETECTORS

Observing the same target with two detectors minimizes the probability of false positives generated by noise and cosmic ray detection. Indeed, those false positive events are unlikely to occur within the same nanosecond on both detectors. We register a *coincidence* if pulses detected on both detectors occurred within the same nanosecond. We record the voltage of the coincidence with the smallest of the two pulse heights during the coincidence. Coincidences are detected by starting to measure the arrival time of each pulse in smoothed waveforms by finding local maxima with first-derivative tests. Then, the data reduction software searches for pulse arrivals between each detector that falls within the same nanosecond.

Assuming that detector noise events (or stellar photo-events) that occur on two detectors are independent, it is possible to predict the coincidence heights from the measured PHDs by using the semi-empirical Wright et al. model[14] based on Poisson statistics. Since the model makes use of experimental PHDs, the predicted coincidence height distribution takes into account both detector noise and stellar photo-detections. Examples of both measured and predicted coincidence height distributions obtained during an acquisition are represented on Fig.3 (respectively in cyan and magenta). The model of coincidences due to detector noise (or star photo-detections) fits the measured coincidence with good agreement. Therefore, a departure from this model of coincidence can alert observers of unexpected events. Right-panel of Fig.3 shows an exceptionally rare high coincidence for which the measured distribution shows a significant departure from the model.

We use the coincidence model at the voltage of the highest detected coincidence to determine the time it takes on average to produce a coincidence from detector and stellar noise. One of our indicators displays that time for each acquisition. This indicator measures how unlikely it was that this coincidence could have been

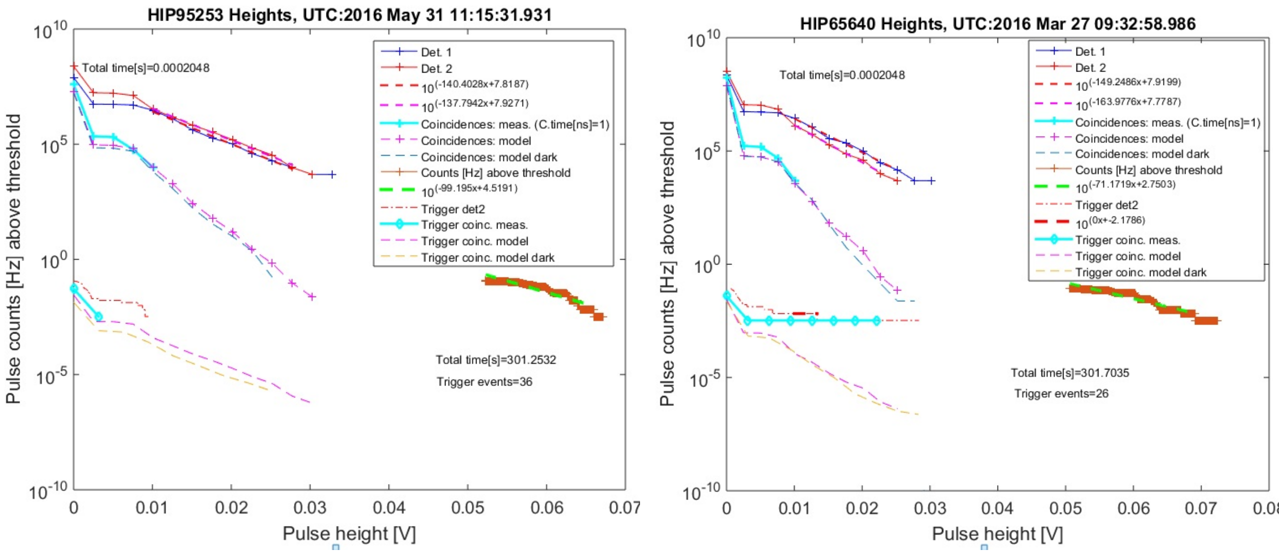

Figure 3: Pulse height and coincident height distributions obtained on two different acquisitions of stars: HIP95253 and HIP65640. Left: Measured coincidences (cyan full line) shows no departure from the model of coincidences produced by detector noise (magenta dashed-dotted line). Right: A large departure from the model was measured revealing that two high pulses occurred within the same nanosecond. The pulses corresponding to this departure event are shown on the right panel of Fig. 2.

due to detector dark noise or stellar photo-detection. A second indicator represents the highest ratio of the measured coincidence distributions to the coincidence distributions predicted by the Wright et al. model, for both waveform and trigger acquisitions.

3.3 FREQUENCY SEARCH: PERIODOGRAMS

We make use of periodograms to search for periodic signals within each detector's smoothed waveform and within the product of the two detector waveforms. The highest peak in the periodogram is identified and compared to the periodogram standard deviation calculated at the middle frequency range. The results are sent to an additional indicator measuring the height of the highest peak in the periodogram in units of standard deviation above the noise. Top panels of Fig. 4 represent periodograms obtained when observing the pulsed laser with detector 1 (left) and detector 2 (right). The frequency comb shows that the periodic signal is easily detectable, and that it matches the exact duty cycle of the pulsed laser emission. Possible high peaks due to persistent sources of instrumental periodic noise can easily be identified if present in dark acquisitions and related frequencies can then be removed from the periodogram peak detections.

3.4 ALARMS & NOTIFICATIONS

We design a set of real-time indicators for observers that summarizes the data analysis for each acquisition (subsections above) to quantify how unlikely were the measured events (e.g., coincidences, pulse heights). For instance, one of these indicators displays the average time it takes to produce the same coincidence if it would have been generated by detector noise (section 3.2). Alarms and notifications are automatically triggered when values are above predefined thresholds to alert observers to potential positive signals or unexpected anomalies in the acquired waveforms. The alarm threshold is set to a 5% probability of having at least one false alarm per 20 acquisitions. For each acquisition, the threshold value is adjusted depending on the exposure time. The notification threshold is set to a 5% probability of having at least one false notification per acquisition. If an alarm or notification is triggered and if the origins of those events can not be identified, re-observations of the same target are performed.

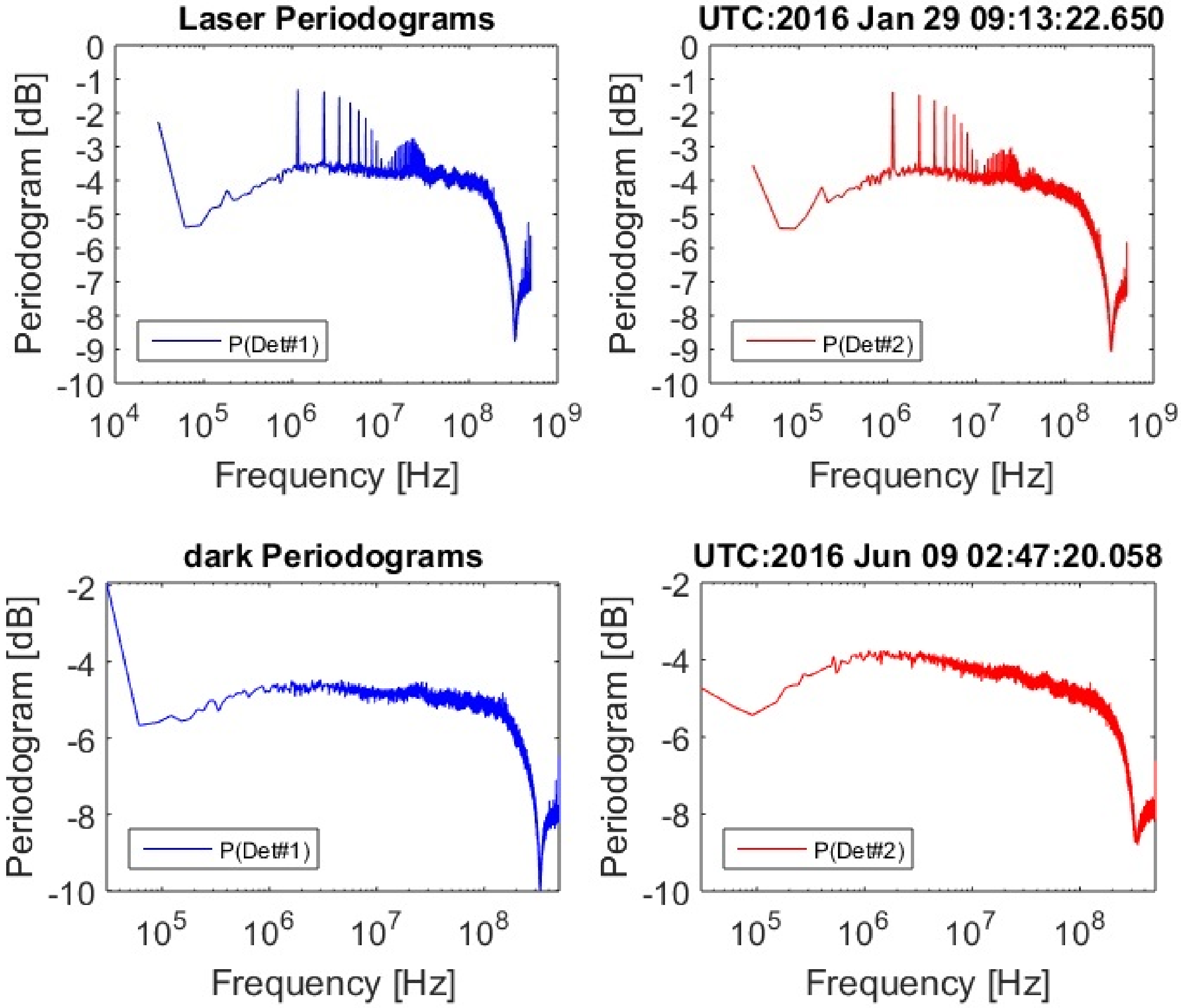

Figure 4: Periodograms obtained by NIROSETI pulsed-laser source observations (top panels) for detector 1 (left) and 2 (right). The pulse-laser calibration unit is easily apparent and detectable in the frequency comb pattern. For comparison, periodograms taken with no light (dark) are represented on the bottom panels.

4. COMMISSIONING AND CALIBRATION PROCEDURES

First light of the instrument was obtained on March 15, 2015 at Lick Observatory. We then commissioned the instrument to ensure that all components were properly installed and operational with the Nickel telescope. Commissioning included verifying the functionality and performance of each device, performing optical alignment, implementing alarm system validation methods, and measuring the instrument sensitivity.

4.1 INSTRUMENTAL ALIGNMENT

Since the instrument includes several focal planes and two detectors with relatively small field-of-view (2.5 arcsec), optical components need to be properly aligned to ensure that the detectors are both receiving light collected by the telescope. For this purpose several stages and kinematic mounts have been implemented to allow on-axis alignment, and tip-tilt orientation of lenses and detectors. The guider camera is mounted on a stage to allow fine tuning of focus differential between detectors and guider camera.

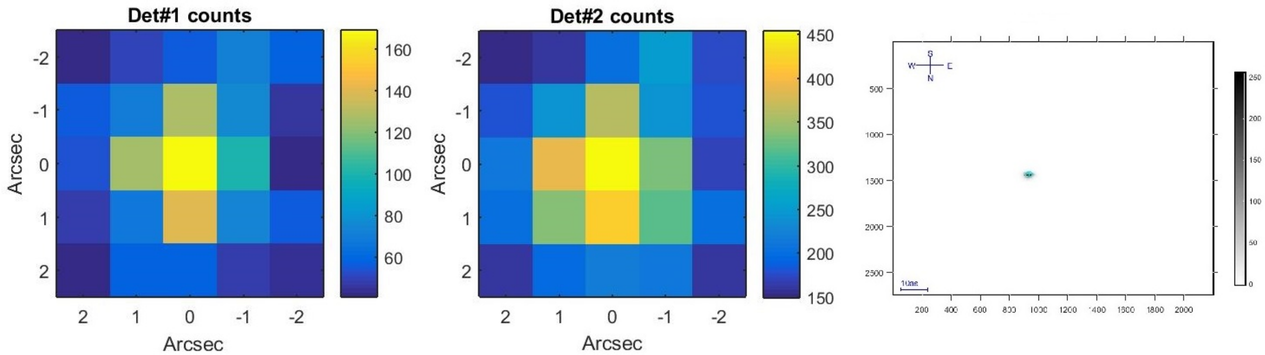

Figure 5: NIROSETI 24μs-exposure 5x5-arcsecond images of HR5226 (left: detector 1, middle: detector 2) obtained simultaneously by dithering the telescope over a square grid pattern with 1-arcsec dither steps. South is up on the plane of the sky. These measurements are essential to test the alignment between both detectors. Right: Guide camera image of HR5226 illustrating how the larger field-of-view guider gives the reference position of the near-infrared. This guider camera reference position is used for acquiring, centering, and guiding on targets to the near-infrared detectors.

At the start of each observing night a specific procedure was implemented to verify the optical alignment of the system. We first observe a bright star and measure the integrated counts of each near-infrared detectors. We then dither the telescope over a 5x5-arcsec field-of-view grid with arcsec steps. As shown on the resulting near-infrared images of Fig.5, detector counts are both maximal in the same pointing direction. This procedure allows alignment within 1-arcsecond accuracy. A 3-arcsec circle is over-plotted on the guider camera image as a reference position for centering and guiding.

During survey observations, the instrument keeps track of alignment by recording pulse counts and acquiring guider images for each target, to verify alignment and telescope pointing. Alignment of the instrument has been found to be very stable over the commissioning and campaign runs, with offset variations between detectors and guider camera smaller than the 1-arcsec resolution.

4.2 CALIBRATION WITH PULSED LASER

A calibration procedure was developed to test the instrument sensitivity and alarm system. A pulsed source unit was built and integrated into the entrance of the instrument to mimic light coming from the telescope with the same focal ratio. Sensitivity testing and alarm system checking are performed on a monthly basis using the pulsed laser source unit.

The 0.98μm wavelength of the pulsed laser diode was chosen for optical alignment, so the light is detectable by both near-infrared detectors and the optical guide camera which has about 4% quantum efficiency at this wavelength. A pulser device with varying duty cycle (in the MHz range) modulates the laser-diode emission to deliver periodic pulses with 10-nanosecond width while also maintaining continuous random laser emissions to mimic background light. Figure 6 shows an example of waveforms obtained when the output optics of the laser source unit is moved onto the instrument optical axis.

We calibrated our laser unit with a set of fiber attenuators by using a fiber-coupled power-meter to quantify the number of photons sent by the laser unit in each pulse. By taking into account instrument throughput and detector efficiency, we measured that a positive detection requires 300 photons per pulse (in its two-detector configuration) at the entrance of the instrument to trigger the alarm system while keeping a low probability of false alarm (5% probability to have a least one false alarm per 20 acquisitions). Therefore, the 1m Nickel telescope needs to receive a 380 ph/m^2/pulse signal to be detected by the instrument. By taking into account 0.2 mag of extinction per kiloparsec at 1.5μm , it can be shown that this instrument mounted on the 1-m telescope can detect a petawatt (or greater) pulsed (nanosecond or smaller) laser located at 50 parsec transmitted with a 10-m class telescope.[8,12]

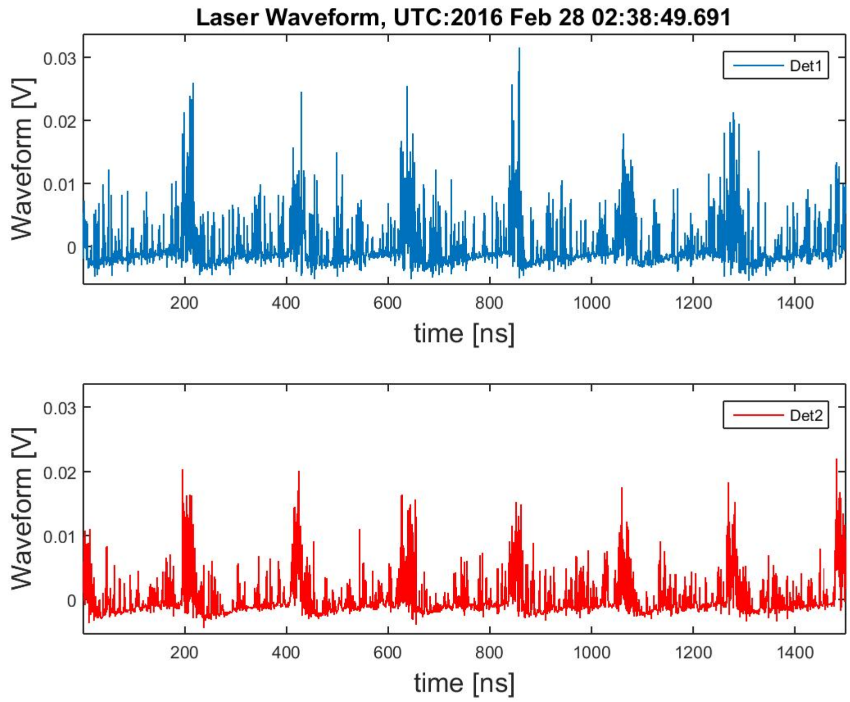

Figure 6: Typical waveforms obtained by observations of the NIROSETI laser source unit which produce 10ns width pulses of light at 0.98μm with a ∼5MHz duty cycle. In addition to these periodic pulses, the laser also produces a specified number of random pulses that can reproduce background star light. The laser source unit is essential for testing the sensitivity of the instrument and data analysis methods.

5. OBSERVATIONAL SETI SURVEY

The NIROSETI survey has been designed for observing several thousand objects over a few years, and commenced operations on January 28th 2016. During a clear night of observations, about 20 to 30 objects are observed after required calibrations such as darks and system alignment tests.

5.1 TARGET SELECTION

The NIROSETI initial target sample contains 1340 objects, mostly main-sequence and giant stars located within 50 parsecs from Earth, drawn from the Breakthrough Listen Program[‡] target list. The NIROSETI list specifically includes all known stars within 5 parsecs observable from Lick Observatory.

A dozen stars known for hosting habitable planets were selected from the Habitable Exoplanets Catalog [§] (virtual Planetary Habitability Laboratory).

Our sample of targets also contains stars that triggered alarms on other targeted SETI surveys.[7,9]

We have also selected 64 stars in the Earth's Transit Zone, where the probability of detecting Earth by use of the transit method is maximal,[16] with stellar distances ranging from 42 to 934 parsecs.

In addition, the survey list contains 82 galaxies that have been selected by the Breakthrough Listen Program for being the nearest representatives of the five major morphological classes of galaxies. Specifically, we have included 20 spirals, 36 ellipticals, 15 dwarf spheroidals, 9 irregulars, and 2 SO galaxies.

‡https://breakthroughinitiatives.org/Initiative/1

§http://phl.upr.edu/projects/habitable-exoplanets-catalog

Twenty-two globular clusters chosen from the Milky Way Star Clusters Catalog[17] were added to our target list. Selected clusters have an average age of stars greater than 1 Giga-year. They are all located within 25 kiloparsecs from Earth and contain at least 50 stars.

5.2 CAMPAIGN DATA STATISTICS

As of June 6th, 2016 the NIROSETI instrument had been used to observe 297 objects (Table 2).

Table 2: Total number of observed objects, alarms and notifications as of June 6th, 2016 (not including calibrations)

Observed objects	Campaign acquisitions	Alarms	Coincidence Notifications	Height Notifications
297	366	1	20	11

An alarm was triggered during HIP65640 observations the night of March 27, 2016 (09:32:59 UT) when the highest coincidence of the campaign was measured. The two coincident pulses obtained with detectors 1 and 2 are shown on the right panel of Figure 2. According to the coincidence occurrence model, this event could occur on average once every 1.4×10^6s (16.07 days) of continuous observations if it was due to detector or stellar noise (Sec.3.2). Although this occurrence time is significantly longer than the 300-s exposure, no alarms were triggered during all re-observations of this object. A total of 20 coincidence notifications (which have a lower threshold than alarm ones) were also generated since the start of the survey. Almost all notifications occurred because of observing very bright stars ($J \leq 0$), which causes the PHD to significantly deviate from the dark PHD. When observing bright stars, detections are stellar-photon limited rather than detector-noise limited. The majority of our target sample have fainter stars ($J > 0$), and are therefore detector-noise limited.

Fig.7 shows the distribution of alarm and indicator values obtained since the survey started. On left of Fig.7 is the distribution of the time it takes on average to obtain the highest measured coincidence for each acquisition, if these events were due solely to detector noise. Distributions are bimodal since all observations include a 0.2ms long exposure waveform acquisition and a 300s data acquisition exposure. As expected, the centers of these bimodal distributions correspond with exposure times. The alarm triggered by observations of HIP65640 is represented by an outlier at 1.4×10^6s (16.07 days). Fig.7 on the right shows the distribution relative to the time it takes on average to produce a pulse having the same height as the highest pulse measured during acquisitions. These distributions are also centered on the 0.2ms and 300s exposure times.

6. SUMMARY

We have generated the first near-infrared SETI instrument and survey using new state-of-the-art near-infrared fast-response APD detectors. We have commissioned the NIROSETI instrument on the 1m Nickel telescope at Lick Observatory, and our SETI survey commenced at the start of 2016. This instrument has enough sensitivity to detect a current-technology laser emission from 50 parsecs away, while maintaining a low false alarm rate using two detectors simultaneously. The NIROSETI survey is targeting stars with a range of spectral types, globular clusters, and nearby galaxies with a range of morphological types.

We developed and implemented advanced data analysis methods that are used in real-time to detect short pulses of near-infrared light emission. If an alarm or notification is triggered, re-observations of the same target is performed. However, we note that a better scenario would be to conduct simultaneous observations of the same target with a second near-infrared instrument located at a different site would give the strongest confirmation of a positive signal. Our team is currently investigating the capability and instrument design of multiple near-infrared instruments and observing locations.

We also plan to expand the NIROSETI applications to other time-domain astrophysical studies. We are interested in implementing a new device in our current instrument that allows absolute timestamps with sub-microsecond resolution. We plan to extend our pulse search to lower time resolutions up to micro-to-milli seconds. We aim to develop new digital signal processing algorithms to search for signals that have varying duty cycles

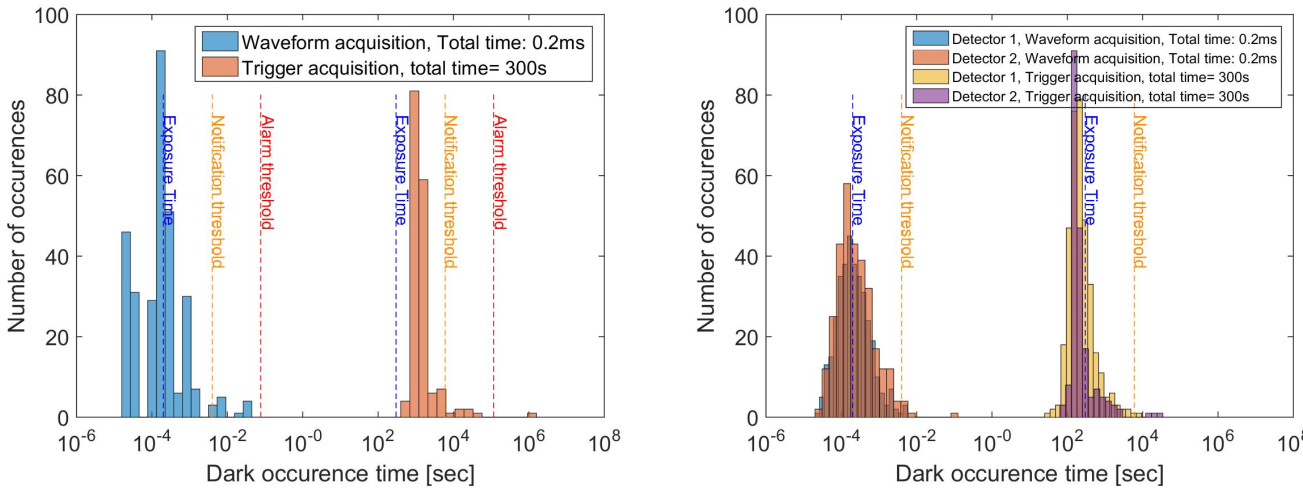

Figure 7: Left: Histogram of the expected occurrence time of the highest coincidence measured during each acquisition. Right: Histogram of the expected occurrence time of the highest pulse height measured on detector 1 and detector 2 for each acquisition.

and pulse widths. All these data analysis methods are beneficial for both optical and infrared SETI, or even other astrophysical programs, that search for *fast* pulses.

ACKNOWLEDGMENTS

We would like to greatly thank the generosity of the Bloomfield Family Foundation for supporting this research and instrument; their interest and enthusiastic support of SETI research catalyzed these endeavors. We would like to extend our thanks to Rafael Ben-Michael, Chief Technology Officer at *Amplification Technologies*, for all the helpful discussions regarding their near-infrared detectors. We would also like to thank the *entire* Lick Observatory staff that supported the successful installation and commissioning of NIROSETI on the Nickel 1m telescope. With special thanks to Lick Observatory and University of California Observatories members: Kostas Chloros, Will Deich, Elinor Gates, Erik Kovacs, Kyle Lancos, Paul Lyman, Camille Martinez, Donnie Redel, Graeme Smith, Shawn Stone and Pavl Zachary. The majority of the laboratory work was carried out at the Dunlap Institute for Astronomy & Astrophysics, University of Toronto. The Dunlap Institute is funded through an endowment established by the David Dunlap family and the University of Toronto.

REFERENCES

[1] Linga, K. R., Krutov, A. V., Godik, E. E., Seemungal, W. A., Shushakov, D., and Shubin, V. E., "Ultra low noise photodetectors with internal discrete amplification," in [*Semiconductor Photodetectors II*], Cohen, M. J. and Dereniak, E. L., eds., *Proc. SPIE* **5726**, 43–51 (Apr. 2005).

[2] Linga, K., Yevtukhov, Y., and Liang, B., "High-gain and low-excess noise near-infrared single-photon avalanche detector arrays," in [*Advanced Photon Counting Techniques IV*], *Proc. SPIE* **7681**, 76810X (Apr. 2010).

[3] Drake, F. D., "How Can We Detect Radio Transmissions from Distant Planetary Systems?," *Sky and Telescope* **19** (Jan. 1960).

[4] Tarter, J., "The Search for Extraterrestrial Intelligence (SETI)," *ARAA* **39**, 511–548 (2001).

[5] Werthimer, D., Anderson, D., Bowyer, C. S., Cobb, J., Heien, E., Korpela, E. J., Lampton, M. L., Lebofsky, M., Marcy, G. W., McGarry, M., and Treffers, D., "Berkeley radio and optical SETI programs: SETI@home, SERENDIP, and SEVENDIP," in [*The Search for Extraterrestrial Intelligence (SETI) in the Optical Spectrum III*], Kingsley, S. A. and Bhathal, R., eds., *Proc. SPIE* **4273**, 104–109 (Aug. 2001).

[6] Horowitz, P., Coldwell, C. M., Howard, A. B., Latham, D. W., Stefanik, R., Wolff, J., and Zajac, J. M., "Targeted and all-sky search for nanosecond optical pulses at Harvard-Smithsonian," in [*The Search for Extraterrestrial Intelligence (SETI) in the Optical Spectrum III*], Kingsley, S. A. and Bhathal, R., eds., *Proc. SPIE* **4273**, 119–127 (Aug. 2001).

[7] Reines, A. E. and Marcy, G. W., "Optical Search for Extraterrestrial Intelligence: A Spectroscopic Search for Laser Emission from Nearby Stars," *PASP* **114**, 416–426 (Apr. 2002).

[8] Howard, A. W., Horowitz, P., Wilkinson, D. T., Coldwell, C. M., Groth, E. J., Jarosik, N., Latham, D. W., Stefanik, R. P., Willman, Jr., A. J., Wolff, J., and Zajac, J. M., "Search for Nanosecond Optical Pulses from Nearby Solar-Type Stars," *ApJ* **613**, 1270–1284 (Oct. 2004).

[9] Stone, R. P. S., Wright, S. A., Drake, F., Muñoz, M., Treffers, R., and Werthimer, D., "Lick Observatory Optical SETI: Targeted Search and New Directions," *Astrobiology* **5**, 604–611 (Oct. 2005).

[10] Siemion, A. P. V., Cobb, J., Chen, H., Cordes, J., Filiba, T., Foster, G., Fries, A., Howard, A., von Korff, J., Korpela, E., Lebofsky, M., McMahon, P. L., Parsons, A., Spitler, L., Wagner, M., and Werthimer, D., "Current and Nascent SETI Instruments," *Proceedings of SETI Sessions at the 2010 Astrobiology Science Conference, Douglas A. Vakoch, Editor* (Sept. 2011).

[11] Tellis, N. K. and Marcy, G. W., "A Search for Optical Laser Emission Using Keck HIRES," *PASP* **127**, 540–551 (June 2015).

[12] Wright, S. A., Werthimer, D., Treffers, R. R., Maire, J., Marcy, G. W., Stone, R. P. S., Drake, F., Meyer, E., Dorval, P., and Siemion, A., "A near-infrared SETI experiment: instrument overview," in [*Ground-based and Airborne Instrumentation for Astronomy V*], *Proc. SPIE* **9147**, 91470J (July 2014).

[13] Mourou, G. A., Korn, G., Sandner, W., and (eds), J. L. C., [*ELI - Extreme Light Infrastructure: Science and Technology with Ultra-Intense Lasers Whitebook*], THOSS Media GmbH (2011).

[14] Wright, S. A., Drake, F., Stone, R. P., Treffers, D., and Werthimer, D., "Improved optical SETI detector," in [*The Search for Extraterrestrial Intelligence (SETI) in the Optical Spectrum III*], Kingsley, S. A. and Bhathal, R., eds., *Proc. SPIE* **4273**, 173–177 (Aug. 2001).

[15] Maire, J., Wright, S. A., Werthimer, D., Treffers, R. R., Marcy, G. W., Stone, R. P. S., Drake, F., and Siemion, A., "A near-infrared SETI experiment: probability distribution of false coincidences," in [*Ground-based and Airborne Instrumentation for Astronomy V*], *Proc. SPIE* **9147**, 91474K (July 2014).

[16] Heller, R. and Pudritz, R. E., "The Search for Extraterrestrial Intelligence in Earth's Solar Transit Zone," *Astrobiology* **16**, 259–270 (Apr. 2016).

[17] Schmeja, S., Kharchenko, N. V., Piskunov, A. E., Röser, S., Schilbach, E., Froebrich, D., and Scholz, R.-D., "Global survey of star clusters in the Milky Way. III. 139 new open clusters at high Galactic latitudes," *Astronomy & Astrophysics* **568**, A51 (Aug. 2014).